Supporting Information

Restructuring of MFI Framework Zeolite Models and Their Associated Artifacts in Density Functional Theory Calculations

Alexander Hoffman, Mykela DeLuca, David Hibbitts*

Department of Chemical Engineering, University of Florida, Gainesville, FL 32601

*corresponding author, hibbitts@che.ufl.edu

Table of Contents

List of Figures

S1. Determination of structural uniqueness using a 3N-dimensional distance

Outputs are structurally indistinguishable and have comparable energy below a threshold value of Δx_{3N}. 3N-dimensional distances were calculated between all Si-forms generated during restructuring through guest species to determine this value. Differences in electronic energies (ΔE_0) tend to increase with distance between structures, but the energy spread—as calculated by RPBE-D[1,2]—for structures where $\Delta x_{3N} > 3$ Å increases rapidly (Figure S1). Previous work[3] has shown that energies of equivalent structures can vary by ~5 kJ mol^{-1} in DFT calculations in zeolites with RPBE-D only by shifting locations of the periodic boundaries.

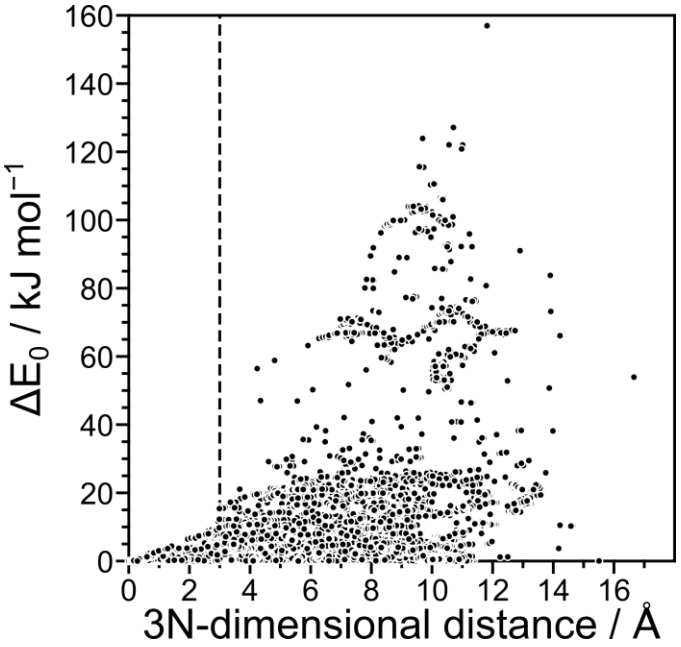

Figure S1. Difference in E_0 with 3N-distance for Si-form structures optimized in RPBE-D. The dashed line shows the distance cutoff at 3 Å.

These data indicate that 3 Å is a serviceable cutoff distance for determining unique or equivalent structures. Table S1 shows the percentage of structures within and outside of this distance of one another that have energy differences less than 1, 5, and 10 kJ mol^{-1}. Nearly all (99.9%) structures within 3 Å of one another have energies within 10 kJ mol^{-1}, and 96.2% of these structures are within 5 kJ mol^{-1}. While there are many structures within 5 and 10 kJ mol^{-1} in energy but differ by $\Delta x_{3N} > 3$ Å, the proportion with energies outside the range of the 5 kJ mol^{-1} DFT error increases dramatically from 3.8% to 49.5%.

Table S1. The percentage of structures within 3 Å of one another and more than 3 Å from one another within 1, 5, and 10 kJ mol^{-1}.

ΔE_0 cutoff kJ mol^{-1}	Structures with $\Delta x_{3N} < 3$ Å %	Structures with $\Delta x_{3N} \geq 3$ Å %
1	65.3	13.8
5	96.2	50.5
10	99.9	73.9

S2. Structural images comparing outputs from each functional

S2.1 Direct optimization of input structures

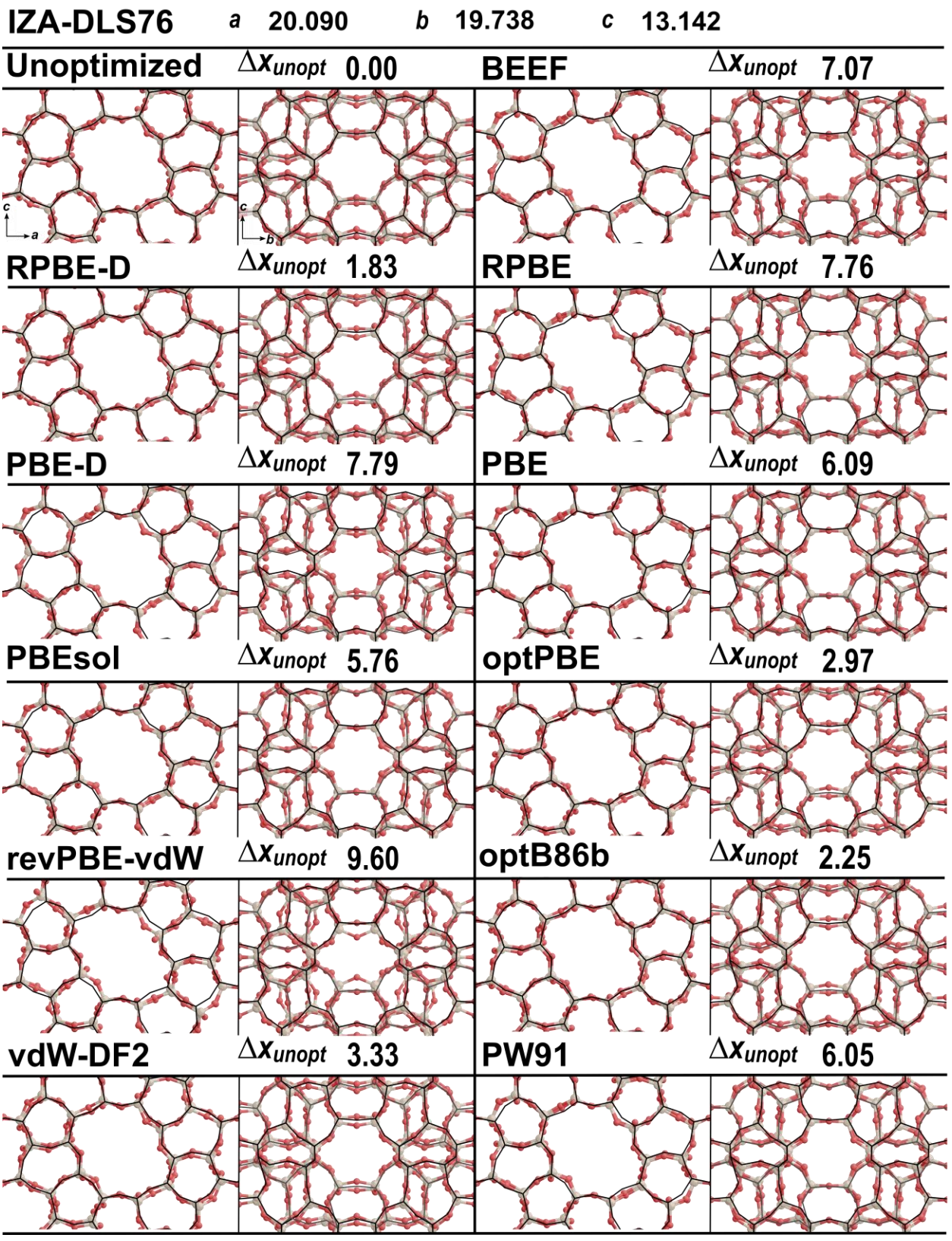

Figure S2. Output structures from direct optimization of the IZA-DLS76 structure. The 3N-dimensional distance between the output and the unoptimized form is shown next to the corresponding functional.

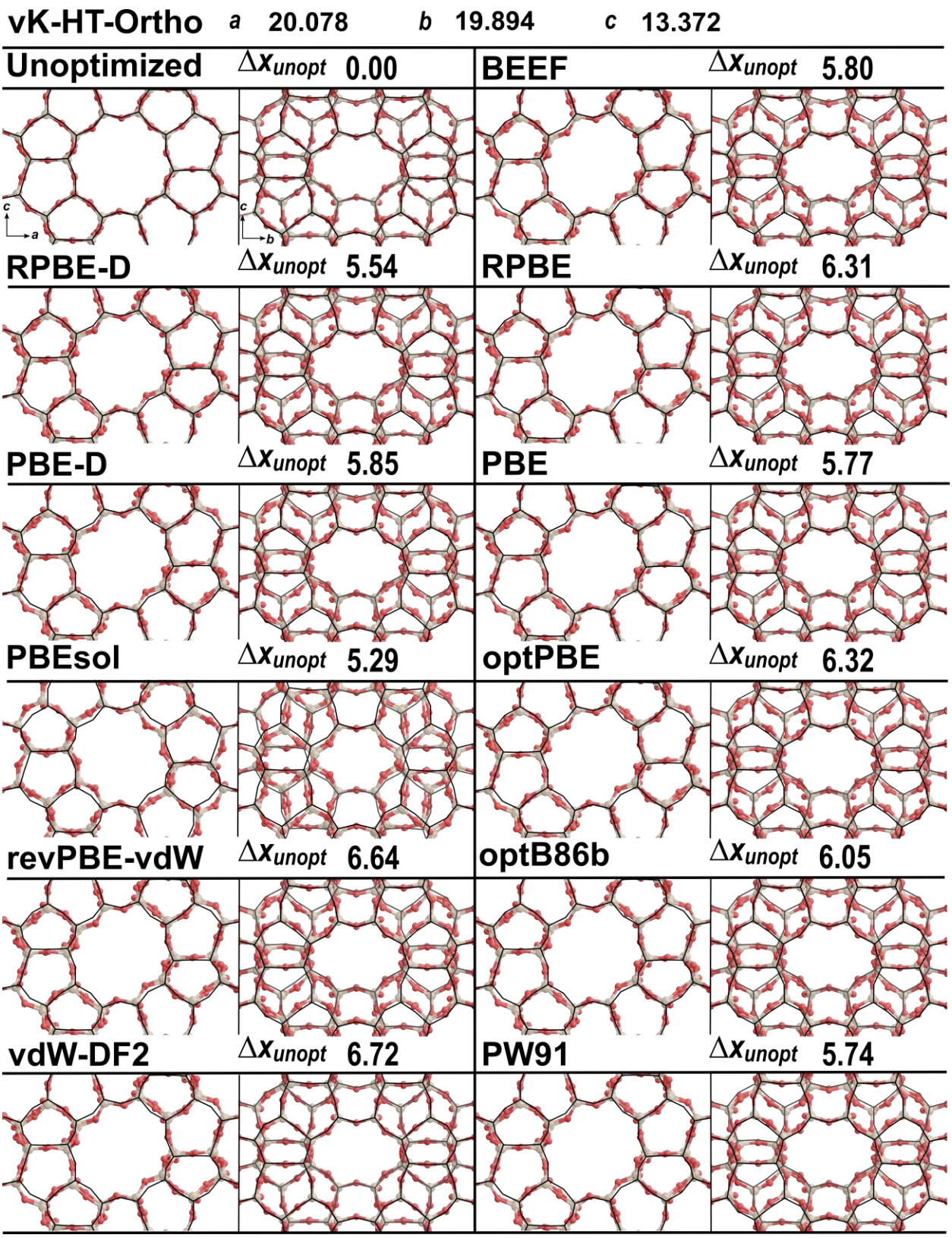

Figure S3. Output structures from direct optimization of the vK-HT-Ortho structure. The 3N-dimensional distance between the output and the unoptimized form is shown next to the corresponding functional.

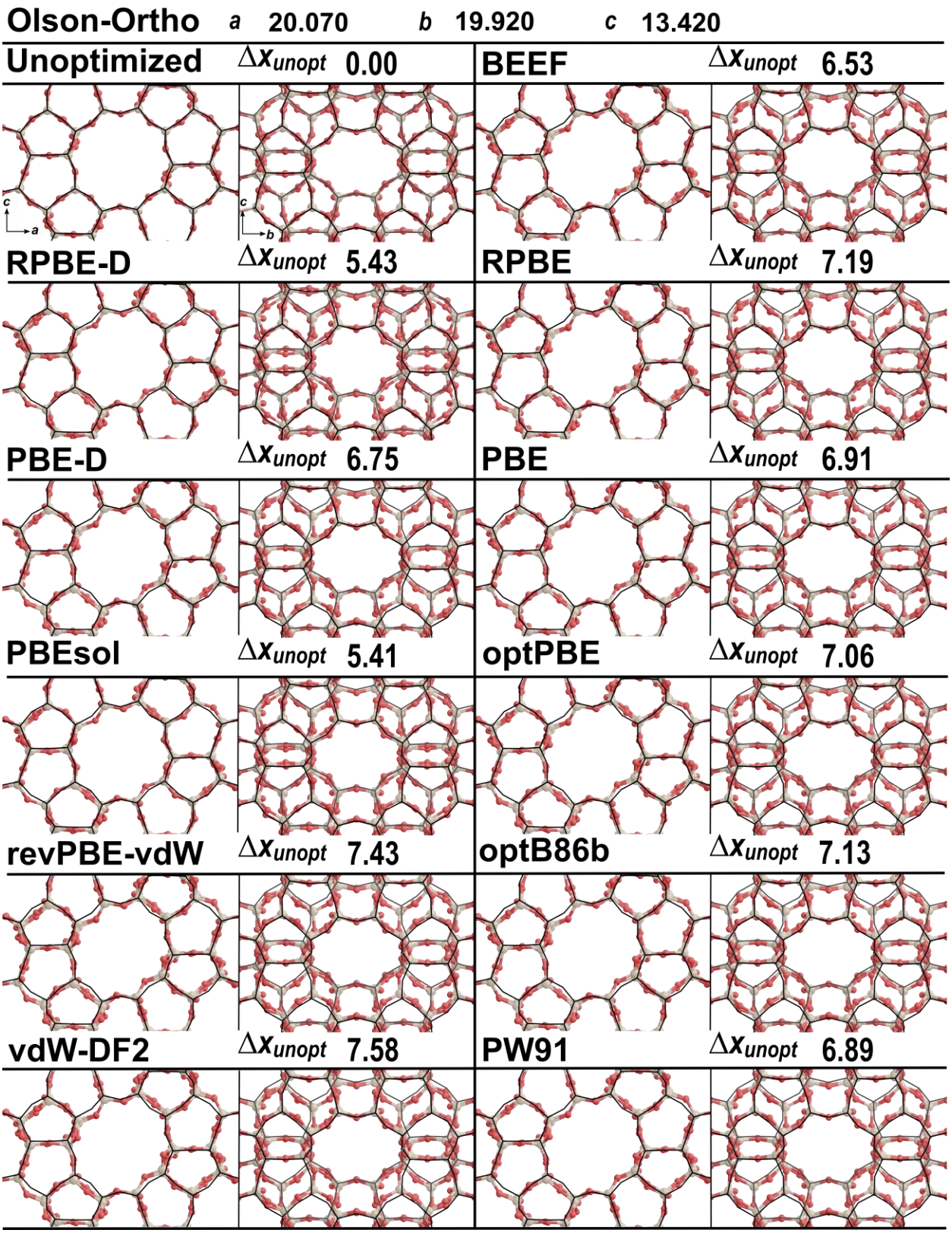

Figure S4. Output structures from direct optimization of the Olson-Ortho structure. The 3N-dimensional distance between the output and the unoptimized form is shown next to the corresponding functional.

S2.2 Post-anneal structures

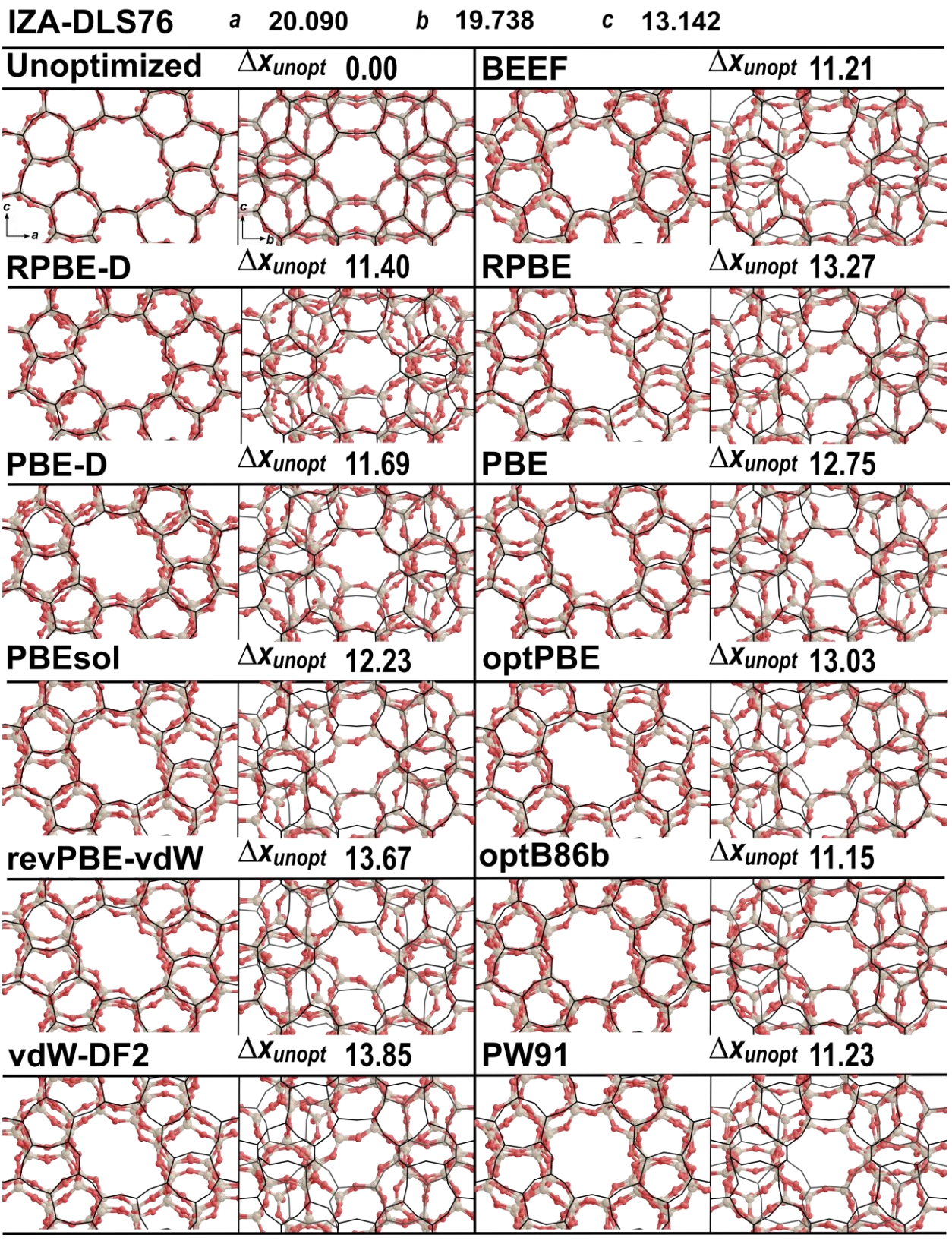

Figure S5. Output structures from post-annealing optimization of the IZA-DLS76 structure. The 3N-dimensional distance between the output and the unoptimized form is shown next to the corresponding functional.

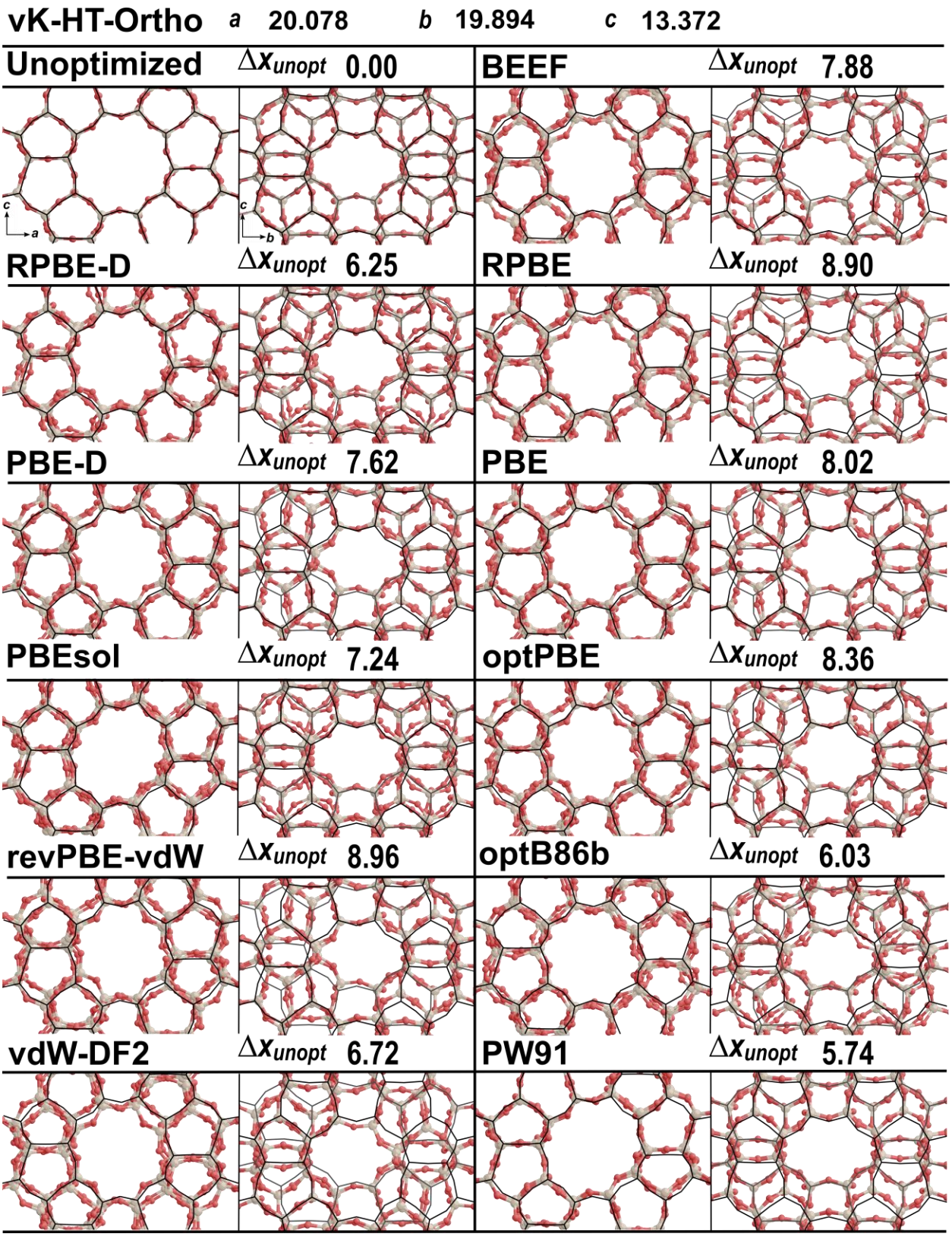

Figure S6. Output structures from post-annealing optimization of the vK-HT-Ortho structure. The 3N-dimensional distance between the output and the unoptimized form is shown next to the corresponding functional.

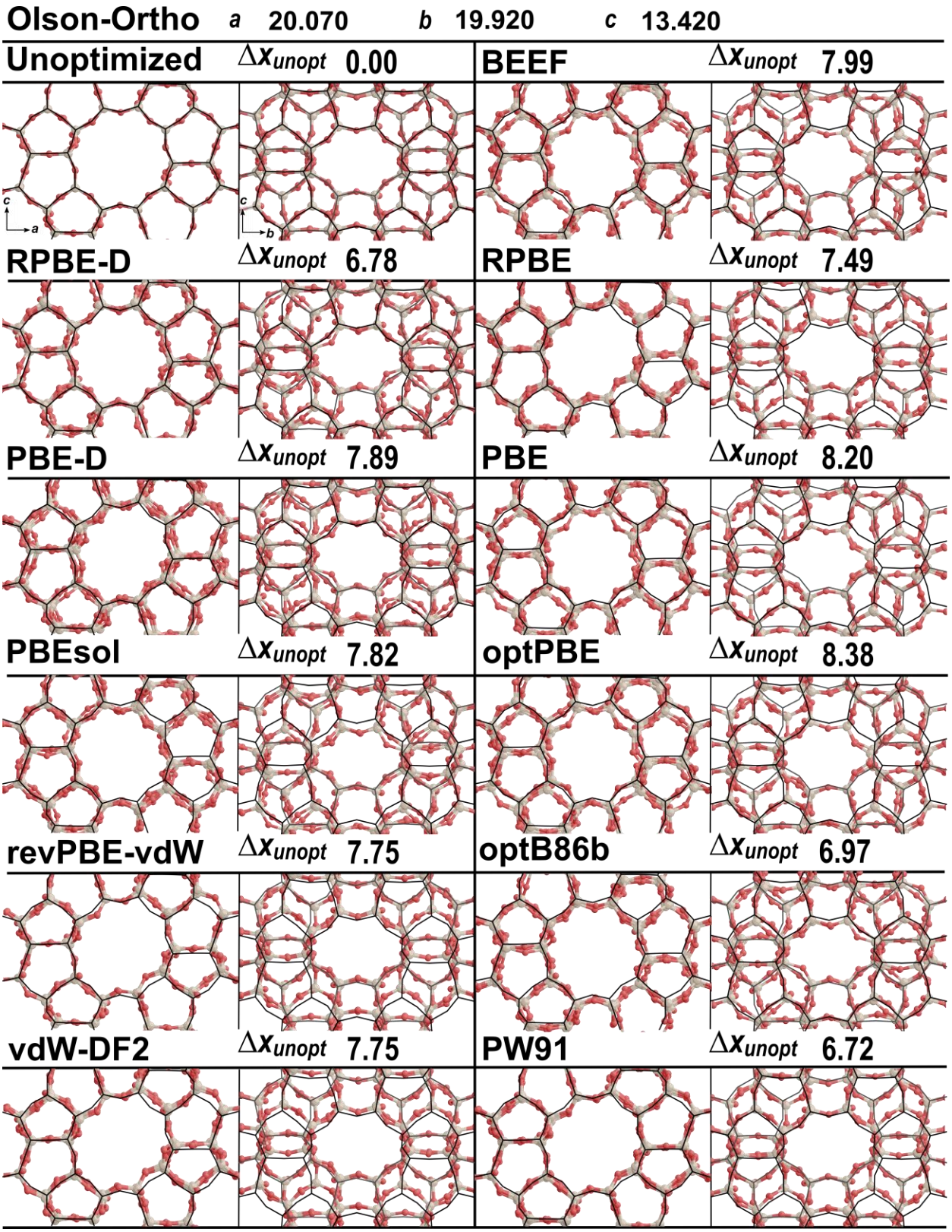

Figure S7. Output structures from post-annealing optimization of the Olson-Ortho structure. The 3N-dimensional distance between the output and the unoptimized form is shown next to the corresponding functional.

S2.3 Post-adsorbate optimization of IZA-DLS76

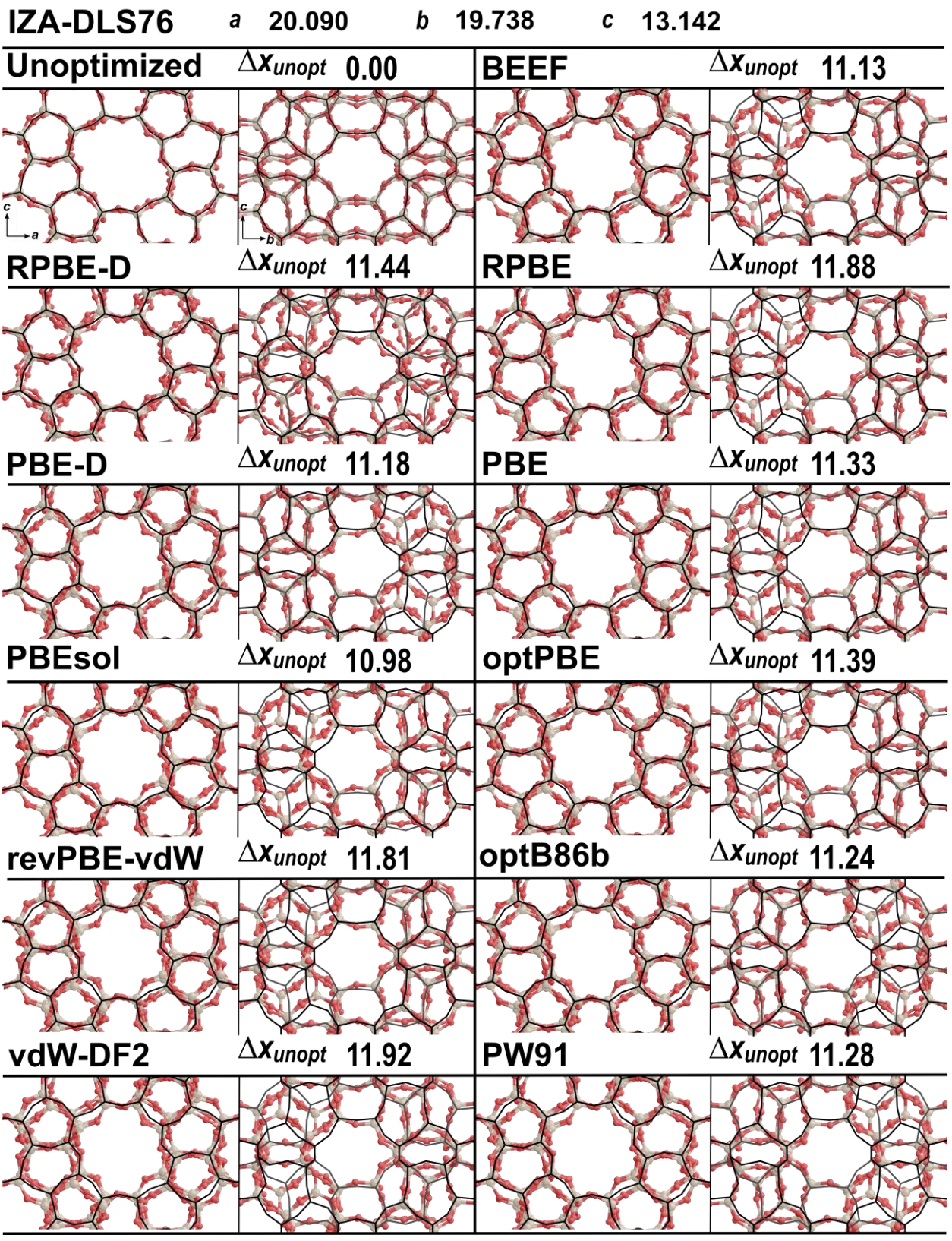

Figure S8. Output structures from post-annealing optimization of the Olson-Ortho structure. The 3N-dimensional distance between the output and the unoptimized form is shown next to the corresponding functional.

S2.4. Structures after unit cell parameter optimization with concurrent atom relaxation

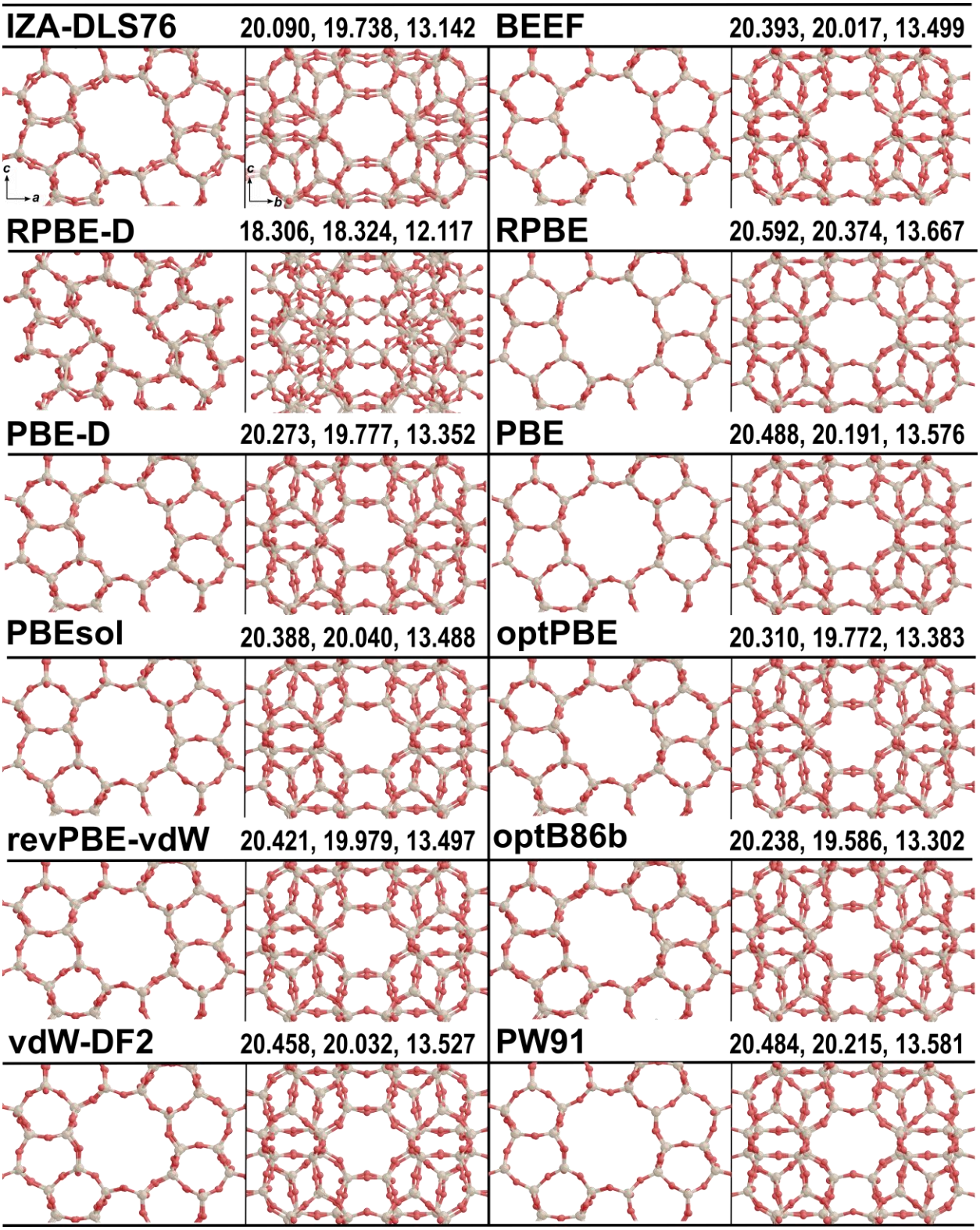

Figure S9. Output structures from unconstrained unit cell parameter optimization of the IZA-DLS76 structure. The final *a*, *b*, and *c* unit cell vector lengths are shown next to the corresponding functional. Angles between vectors are summarized in Table S5.

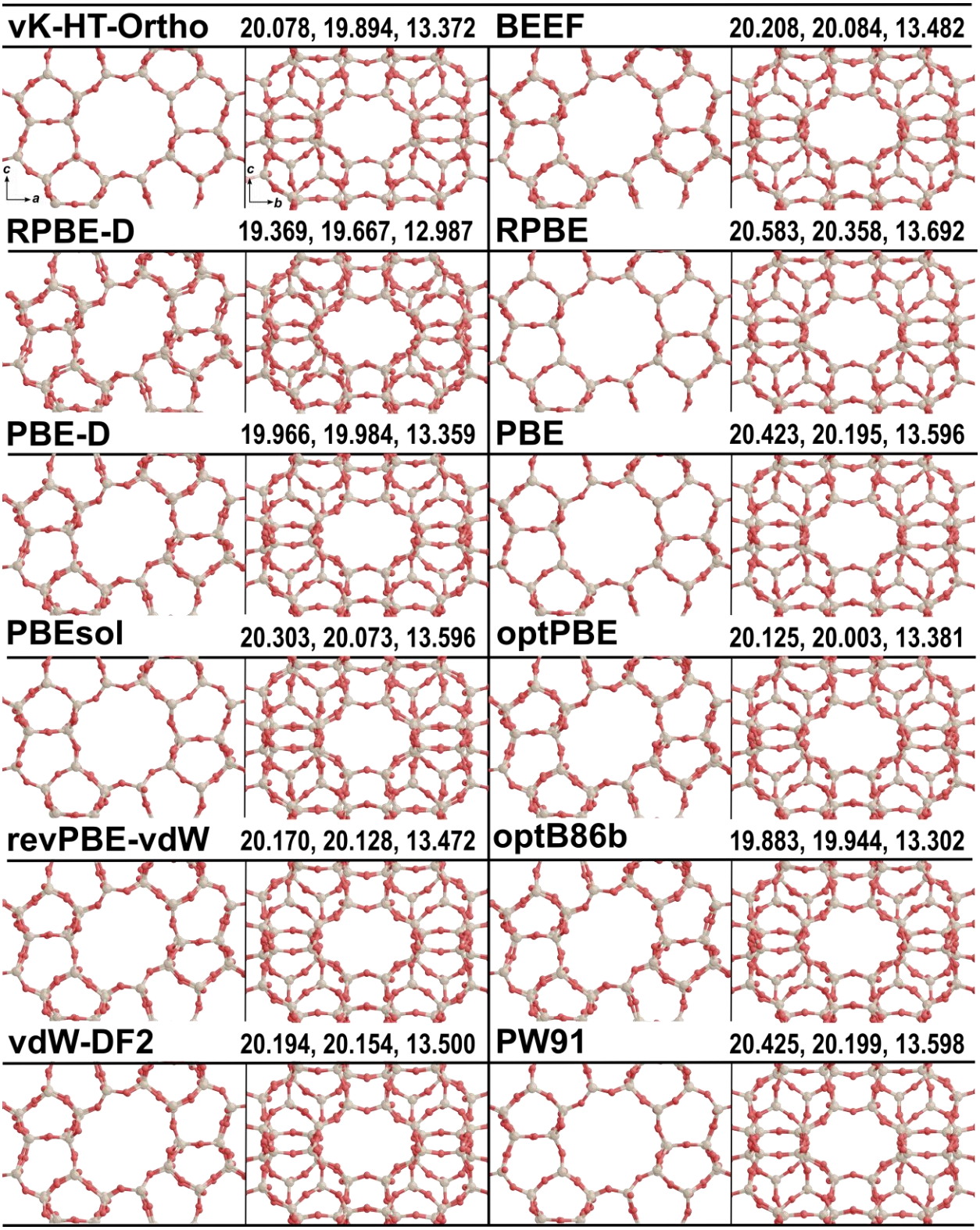

Figure S10. Output structures from unconstrained unit cell parameter optimization of the vK-HT-Ortho structure. The final *a*, *b*, and *c* unit cell vector lengths are shown next to the corresponding functional. Angles between vectors are summarized in Table S5.

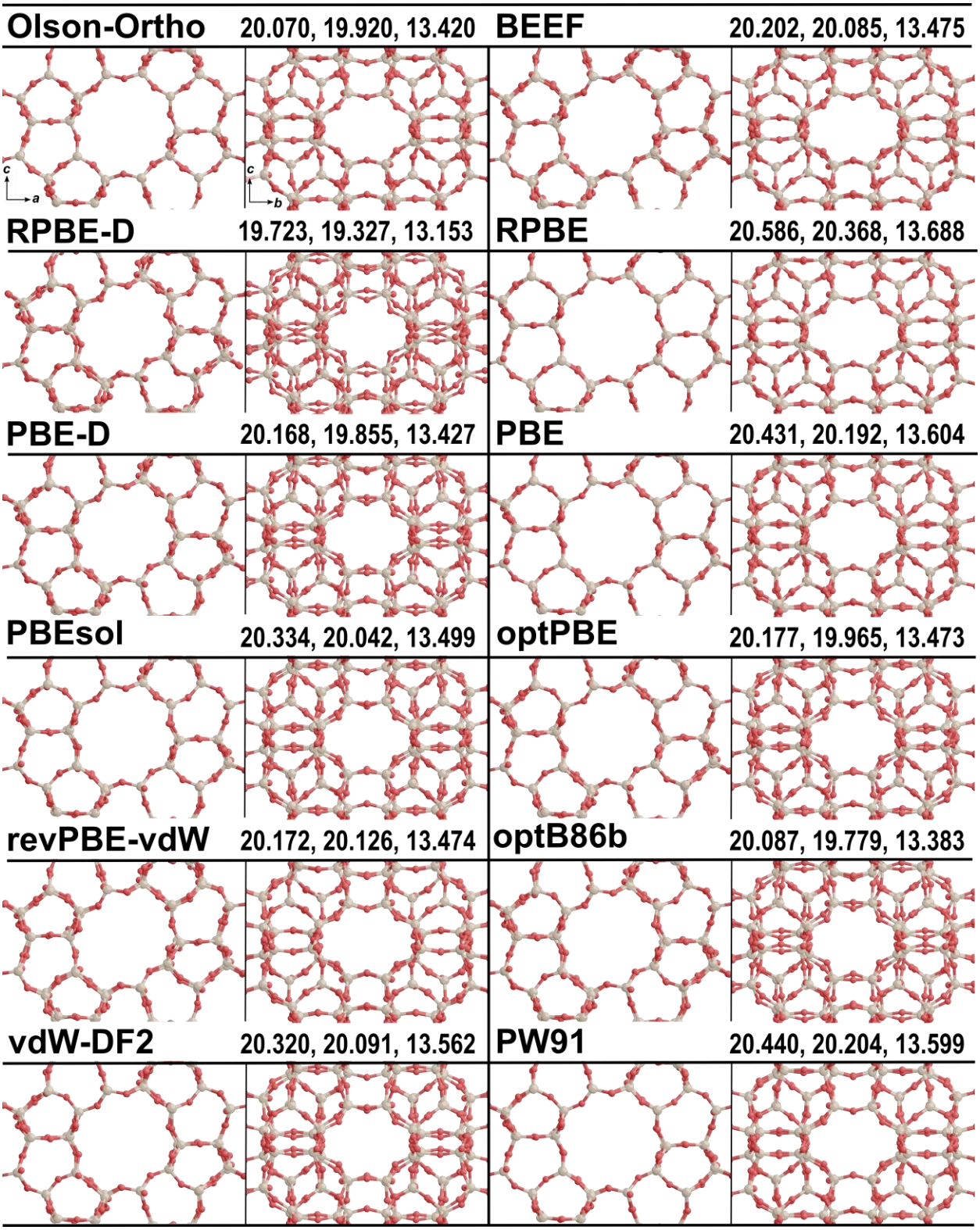

Figure S11. Output structures from unconstrained unit cell parameter optimization of the Olson-Ortho structure. The final *a*, *b*, and *c* unit cell vector lengths are shown next to the corresponding functional. Angles between vectors are summarized in Table S5.

S3. Structural information for optimized MFI frameworks

Table S2. Si–O bond lengths and Si–O–Si bond angles for unoptimized structures and structures optimized in each exchange-correlation functional scheme tested.

Functional	Framework	Average Si–O Bond Length	Average Si–O–Si Bond Angle
		Å	°
(Unoptimized)	IZA-DLS76[a]	1.610	148.076
	vK-HT-Ortho[b]	1.587	156.015
	Olson-Ortho[c]	1.592	155.494
BEEF	IZA-DLS76	1.624	144.937
	vK-HT-Ortho	1.627	145.137
	Olson-Ortho	1.626	146.430
RPBE-D	IZA-DLS76	1.624	144.937
	vK-HT-Ortho	1.627	145.137
	Olson-Ortho	1.626	146.430
RPBE	IZA-DLS76	1.628	146.543
	vK-HT-Ortho	1.628	146.015
	Olson-Ortho	1.628	146.513
PBE-D	IZA-DLS76	1.622	146.661
	vK-HT-Ortho	1.623	146.628
	Olson-Ortho	1.623	147.192
PBE	IZA-DLS76	1.622	146.921
	vK-HT-Ortho	1.623	146.907
	Olson-Ortho	1.623	147.509
PBEsol	IZA-DLS76	1.618	147.225
	vK-HT-Ortho	1.618	147.730
	Olson-Ortho	1.618	147.934
optPBE	IZA-DLS76	1.626	145.625
	vK-HT-Ortho	1.627	145.850
	Olson-Ortho	1.627	146.322
revPBE-vdW	IZA-DLS76	1.631	146.065
	vK-HT-Ortho	1.631	145.307
	Olson-Ortho	1.631	145.307
optB86b	IZA-DLS76	1.623	145.907
	vK-HT-Ortho	1.624	146.284

	Olson-Ortho	1.624	146.914
vdW-DF2	IZA-DLS76	1.629	145.202
	vK-HT-Ortho	1.630	145.421
	Olson-Ortho	1.630	145.884
PW91	IZA-DLS76	1.621	147.102
	vK-HT-Ortho	1.621	147.271
	Olson-Ortho	1.622	147.896

[a] The unit cell parameters of IZA-DLS76 are *a*=20.090 Å, *b*=19.738 Å, *c*= 13.142 Å, α=β=γ=90.0°. [b] The unit cell parameters of vK-HT-Ortho are *a*=20.078 Å, *b*=19.894 Å, *c*= 13.372 Å, α=β=γ=90.0°. [c] The unit cell parameters of Olson-Ortho are *a*=20.07 Å, *b*=19.92 Å, *c*= 13.42 Å, α=β=γ=90.0°.

Table S3. Si–O bond lengths and Si–O–Si bond angles for each unoptimized structure and structures after unit cell parameter optimization with atomic positions and unit cell vector angles constrained (ISIF=7) in each exchange-correlation functional scheme tested.

Functional	Framework	Avg. Si–O Bond Length	Avg. Si–O–Si Bond Angle	Unit Cell Parameters		
				a	*b*	*c*
		Å	°	*Å*		
(Unoptimized)	IZA-DLS76[a]	1.610	148.076	20.090	19.738	13.142
	vK-HT-Ortho	1.587	156.015	20.078	19.894	13.372
	Olson-Ortho	1.592	155.494	20.070	19.920	13.420
BEEF	IZA-DLS76	1.6242	147.219	20.090	19.738	13.142
	vK-HT-Ortho	1.6234	147.1702	20.078	19.894	13.372
	Olson-Ortho	1.623	147.6696	20.070	19.920	13.420
RPBE-D	IZA-DLS76	1.6211	144.9366	20.090	19.738	13.142
	vK-HT-Ortho	1.6206	145.1374	20.078	19.894	13.372
	Olson-Ortho	1.6202	146.4304	20.070	19.920	13.420
RPBE	IZA-DLS76	1.6351	146.5428	20.090	19.738	13.142
	vK-HT-Ortho	1.6347	146.0145	20.078	19.894	13.372
	Olson-Ortho	1.6344	146.5134	20.070	19.920	13.420
PBE-D	IZA-DLS76	1.6236	146.6605	20.090	19.738	13.142
	vK-HT-Ortho	1.6227	146.6277	20.078	19.894	13.372
	Olson-Ortho	1.6223	147.1916	20.090	19.738	13.142
PBE	IZA-DLS76	1.6271	146.921	20.090	19.738	13.142
	vK-HT-Ortho	1.6265	146.9066	20.078	19.894	13.372
	Olson-Ortho	1.6261	147.5089	20.070	19.920	13.420

PBEsol	IZA-DLS76	1.6207	147.2247	20.090	19.738	13.142		
	vK-HT-Ortho	1.6199	147.7302	20.078	19.894	13.372		
	Olson-Ortho	1.6194	148.9337	20.070	19.920	13.420		
optPBE	IZA-DLS76	1.6283	145.625	20.090	19.738	13.142		
	vK-HT-Ortho	1.6276	145.8502	20.078	19.894	13.372		
	Olson-Ortho	1.6273	146.3224	20.070	19.920	13.420		
revPBE-vdW	IZA-DLS76	1.6332	146.0652	20.090	19.738	13.142		
	vK-HT-Ortho	1.6331	145.3065	20.078	19.894	13.372		
	Olson-Ortho	1.6328	145.7452	20.090	19.738	13.142		
optB86b	IZA-DLS76	1.624	145.9066	20.090	19.738	13.142		
	vK-HT-Ortho	1.6233	146.2839	20.078	19.894	13.372		
	Olson-Ortho	1.6229	146.9143	20.070	19.920	13.420		
vdW-DF2	IZA-DLS76	1.6342	145.2019	20.090	19.738	13.142		
	vK-HT-Ortho	1.6334	145.4208	20.078	19.894	13.372		
	Olson-Ortho	1.6331	145.8835	20.070	19.920	13.420		
PW91	IZA-DLS76	1.6258	147.102	20.090	19.738	13.142		
	vK-HT-Ortho	1.6252	147.2706	20.078	19.894	13.372		
	Olson-Ortho	1.6247	147.8959	20.070	19.920	13.420		

[a] The fixed unit cell parameters of all three frameworks (IZA-DLS76, vK-HT-Ortho, and OlsonOrtho) are α=β=γ=90.0°.

Table S4. Si–O bond lengths and Si–O–Si bond angles for unoptimized structures and structures after unit cell parameter optimization with atomic positions constrained but without shape constraints (ISIF=6) in each exchange-correlation functional scheme tested.

Functional	Framework	Avg. Si–O Bond Length	Avg. Si–O–Si Bond Angle	Unit Cell Parameters					
				a	*b*	*c*	*α*	*β*	*γ*
		Å	°	*Å*			°		
(Unoptimized)	IZA-DLS76	1.610	148.076	20.090	19.738	13.142	90.000	90.000	90.000
	vK-HT-Ortho	1.587	156.015	20.078	19.894	13.372	90.000	90.000	90.000
	Olson-Ortho	1.592	155.494	20.070	19.920	13.420	90.000	90.000	90.000
BEEF	IZA-DLS76	1.6242	147.219	20.090	19.738	13.142	89.9999	90.0000	90.0001
	vK-HT-Ortho	1.6234	147.1702	20.078	19.894	13.372	90.0001	90.0001	90.0001
	Olson-Ortho	1.623	147.6696	20.070	19.920	13.420	89.9999	90.0000	90.0001
RPBE-D	IZA-DLS76	1.6211	144.9366	20.090	19.738	13.142	90.0000	90.0000	90.0001
	vK-HT-Ortho	1.6206	145.1374	20.078	19.894	13.372	90.0000	90.0000	90.0000
	Olson-Ortho	1.6202	146.4304	20.070	19.920	13.420	90.0001	90.0000	90.0001

	IZA-DLS76	1.6351	146.5428	20.090	19.738	13.142	90.0000	90.0000	89.9998
RPBE	vK-HT-Ortho	1.6347	146.0145	20.078	19.894	13.372	90.0001	89.9999	90.0000
	Olson-Ortho	1.6344	146.5134	20.070	19.920	13.420	89.9998	90.0001	89.9999
	IZA-DLS76	1.6236	146.6605	20.090	19.738	13.142	89.9999	90.0001	89.9999
PBE-D	vK-HT-Ortho	1.6227	146.6277	20.078	19.894	13.372	90.0000	90.0000	90.0001
	Olson-Ortho	1.6223	147.1916	20.070	19.920	13.420	90.0002	90.0000	90.0001
	IZA-DLS76	1.6271	146.921	20.090	19.738	13.142	89.9999	90.0001	89.9999
PBE	vK-HT-Ortho	1.6265	146.9066	20.078	19.894	13.372	90.0001	89.9999	90.0001
	Olson-Ortho	1.6261	147.5089	20.070	19.920	13.420	89.9999	89.9999	90.0002
	IZA-DLS76	1.6207	147.2247	20.090	19.738	13.142	89.9999	89.9999	90.0001
PBEsol	vK-HT-Ortho	1.6199	147.7302	20.078	19.894	13.372	90.0000	90.0000	90.0000
	Olson-Ortho	1.6194	148.9337	20.070	19.920	13.420	90.0000	90.0000	90.0000
	IZA-DLS76	1.6283	145.625	20.090	19.738	13.142	89.9999	89.9999	89.9999
optPBE	vK-HT-Ortho	1.6276	145.8502	20.078	19.894	13.372	90.0000	90.0000	90.0000
	Olson-Ortho	1.6273	146.3224	20.070	19.920	13.420	89.9998	90.0001	90.0001
	IZA-DLS76	1.6332	146.0652	20.090	19.738	13.142	89.9999	90.0001	89.9998
revPBE-vdW	vK-HT-Ortho	1.6331	145.3065	20.078	19.894	13.372	90.0000	89.9999	90.0000
	Olson-Ortho	1.6328	145.7452	20.070	19.920	13.420	89.9999	90.0000	90.0001
	IZA-DLS76	1.624	145.9066	20.090	19.738	13.142	90.0000	90.0000	89.9999
optB86b	vK-HT-Ortho	1.6233	146.2839	20.070	19.920	13.420	89.9998	89.9999	90.0000
	Olson-Ortho	1.6229	146.9143	20.078	19.894	13.372	90.0001	90.0001	90.0000
	IZA-DLS76	1.6342	145.2019	20.090	19.738	13.142	90.0001	89.9999	90.0000
vdW-DF2	vK-HT-Ortho	1.6334	145.4208	20.078	19.894	13.372	89.9999	90.0000	90.0000
	Olson-Ortho	1.6331	145.8835	20.070	19.920	13.420	89.9998	90.0000	89.9999
	IZA-DLS76	1.6258	147.102	20.090	19.738	13.142	90.0000	90.0000	89.9999
PW91	vK-HT-Ortho	1.6252	147.2706	20.078	19.894	13.372	90.0000	90.0001	89.9998
	Olson-Ortho	1.6247	147.8959	20.070	19.920	13.420	90.0000	90.0001	90.0001

Table S5. Si–O bond lengths and Si–O–Si bond angles for unoptimized structures and structures after unconstrained unit cell parameter optimization (ISIF=3) in each exchange-correlation functional scheme tested.

Functional	Framework	Avg. Si–O Bond Length	Avg. Si–O–Si Bond Angle	Unit Cell Parameters					
				a	*b*	*c*	*α*	*β*	*γ*
		Å	°	*Å*				°	
	IZA-DLS76	1.610	148.076	20.090	19.738	13.142	90.000	90.000	90.000

(Unoptimized)	vK-HT-Ortho	1.587	156.015	20.078	19.894	13.372	90.000	90.000	90.000
	Olson-Ortho	1.592	155.494	20.070	19.920	13.420	90.0000	90.000	90.000
	IZA-DLS76	1.621	151.647	20.371	20.064	13.485	90.0033	89.9970	89.9953
BEEF	vK-HT-Ortho	1.622	149.847	20.208	20.084	13.482	90.0007	90.0010	90.0008
	Olson-Ortho	1.622	149.781	20.202	20.085	13.475	90.0005	90.0013	89.9994
	IZA-DLS76	1.621	134.277	18.306	18.324	12.117	90.0000	90.0000	90.0000
RPBE-D	vK-HT-Ortho	1.625	139.216	19.369	19.667	12.987	89.9975	89.9994	90.0006
	Olson-Ortho	1.624	141.332	19.723	19.327	13.153	90.0066	90.0006	90.0002
	IZA-DLS76	1.629	154.890	20.592	20.374	13.667	90.0009	90.0060	89.9996
RPBE	vK-HT-Ortho	1.629	154.770	20.583	20.358	13.692	90.0003	89.9993	90.0001
	Olson-Ortho	1.629	154.893	20.586	20.368	13.688	90.0003	89.9997	89.9999
	IZA-DLS76	1.622	148.742	20.273	19.777	13.352	90.0013	89.9802	90.0066
PBE-D	vK-HT-Ortho	1.623	146.790	19.966	19.984	13.359	89.9991	90.0041	90.0003
	Olson-Ortho	1.622	148.507	20.168	19.855	13.427	90.0097	90.0062	90.0003
	IZA-DLS76	1.623	153.473	20.488	20.191	13.576	90.0009	90.0000	89.9982
PBE	vK-HT-Ortho	1.623	152.899	20.423	20.195	13.596	90.0002	90.0024	89.9998
	Olson-Ortho	1.623	153.121	20.431	20.192	13.604	90.0013	90.0001	90.0000
	IZA-DLS76	1.618	152.330	20.388	20.040	13.488	90.0035	89.9822	90.0086
PBEsol	vK-HT-Ortho	1.618	151.818	20.303	20.073	13.515	90.0001	90.0001	90.0003
	Olson-Ortho	1.618	151.855	20.334	20.042	13.499	89.9993	90.0003	90.0002
	IZA-DLS76	1.627	148.363	20.310	19.772	13.383	90.0005	89.9961	89.9995
optPBE	vK-HT-Ortho	1.627	146.626	20.125	20.003	13.381	90.0009	90.0014	90.0005
	Olson-Ortho	1.627	148.085	20.177	19.965	13.473	89.9996	90.0000	89.9998
	IZA-DLS76	1.631	149.789	20.421	19.979	13.497	89.9980	90.0012	89.9975
revPBE-vdW	vK-HT-Ortho	1.631	147.751	20.170	20.128	13.472	90.0003	90.0006	89.9982
	Olson-Ortho	1.631	147.757	20.172	20.126	13.474	90.0036	89.9995	89.9994
	IZA-DLS76	1.624	147.338	20.238	19.586	13.302	89.9991	89.9994	90.0274
optB86b	vK-HT-Ortho	1.624	145.406	19.883	19.944	13.302	89.9990	90.0082	90.0003
	Olson-Ortho	1.623	147.149	20.087	19.779	13.383	90.0002	90.0045	90.0000
	IZA-DLS76	1.631	150.410	20.458	20.032	13.527	89.9998	90.0014	90.0009
vdW-DF2	vK-HT-Ortho	1.631	148.345	20.194	20.154	13.500	90.0006	90.0093	89.9993

	Olson-Ortho	1.631	149.716	20.320	20.091	13.562	90.0010	89.9998	89.9997
	IZA-DLS76	1.621	154.037	20.484	20.215	13.581	90.0011	89.9981	89.9995
PW91	vK-HT-Ortho	1.622	153.320	20.425	20.199	13.598	90.0004	89.9996	89.9992
	Olson-Ortho	1.622	153.629	20.440	20.204	13.599	90.0000	89.9991	90.0002

S4. Formation energies for directly optimized vK-HT-Ortho from α-quartz

Table S6 shows the energy to form MFI from α-quartz based on the calculated energy for the directly optimized vK-HT-Ortho structure in each functional scheme tested here. These calculated values are compared to experimental formation enthalpies.[4] Previous work has shown that DFT-calculated electronic energies are adequate approximations for formation enthalpies for zeolites from α-quartz, and are better approximated by dispersion corrected DFT calculations, which are corroborated by these results.[5,6] There are, however, no clear trends between the formation energies from α-quartz shown here and the spread in energies of restructured MFI forms shown in our work. There are also no trends with changes in unit cell volume which occurs during simultaneous optimization of unit cell parameters and atomic positions.

Table S6. DFT-calculated energies of formation for the directly optimized vK-HT-Ortho MFI from α-quartz.

	Formation E_0 per unit cell Si (kJ mol^{-1})		
Functional Scheme	IZA-DLS76	vK-HT-Ortho	Olson-Ortho
Experimental, MFI/F[a]	6.8±0.8		
Experimental, MFI/OH[a]	8.01±0.82		
BEEF	8.82	7.66	7.53
RPBE-D	9.17	8.55	9.03
RPBE	0.77	-1.00	-1.27
PBE-D	9.21	8.49	8.46
PBE	2.31	0.92	0.73
PBEsol	2.34	1.40	1.42
optPBE-vdW	12.41	11.03	10.97
revPBE-vdW	11.13	10.02	9.89
optB86b-vdW	11.70	10.61	10.60
vdW-DF2	11.66	9.85	9.69
PW91	2.18	0.82	0.64

[a]Values taken from reference 4 below.

References

(1) Hammer, B.; Hansen, L. B.; Nørskov, J. K. Improved Adsorption Energetics Within Density-functional Theory Using Revised Perdew-Burke-Ernzerhof Functionals. *Phys. Rev. B* **1999**, *59*, 7413–7421.

(2) Grimme, S.; Ehrlich, S.; Goerigk, L. Effect of the Damping Function in Dispersion Corrected Density Functional Theory. *J. Comput. Chem.* **2011**, *32*, 1456–1465.

(3) Nystrom, S.; Hoffman, A.; Hibbitts, D. Tuning Brønsted Acid Strength by Altering Site Proximity in CHA Framework Zeolites. *ACS Catal.* **2018**.

(4) Navrotsky, A.; Trofymluk, O.; Levchenko, A. A. Thermochemistry of Microporous and Mesoporous Materials. *Chem. Rev.* **2009**, *109*, 3885–3902.

(5) Román-Román, E. I.; Zicovich-Wilson, C. M. The Role of Long-range van Der Waals Forces in the Relative Stability of SiO2-zeolites. *Chem. Phys. Lett.* **2015**, *619*, 109–114.

(6) Fischer, M.; Evers, F. O.; Formalik, F.; Olejniczak, A. Benchmarking DFT-GGA Calculations for the Structure Optimisation of Neutral-framework Zeotypes. *Theor. Chem. Acc.* **2016**, *135*, 257.